Trk receptor signalling and sensory neuron fate are perturbed in human neuropathy caused by *Gars* mutations

Running title: Sensory neuron identity is impaired in CMT2D mice

James N. Sleigh[1,*], John M. Dawes[2,#], Steven J. West[2,#], Na Wei[3], Emily L. Spaulding[4,5], Adriana Gómez-Martín[1], Qian Zhang[3], Robert W. Burgess[4,5], M. Zameel Cader[2], Kevin Talbot[2], Xiang-Lei Yang[3], David L. Bennett[2], Giampietro Schiavo[1,*]

[1] Sobell Department of Motor Neuroscience and Movement Disorders, Institute of Neurology, University College London, London WC1N 3BG, UK

[2] Nuffield Department of Clinical Neurosciences, University of Oxford, John Radcliffe Hospital, Oxford OX3 9DU, UK.

[3] Departments of Chemical Physiology and Cell and Molecular Biology, The Scripps Research Institute, La Jolla, California 92037, USA.

[4] The Jackson Laboratory, Bar Harbor, ME 04609, USA.

[5] The Graduate School of Biomedical Science and Engineering, The University of Maine, Orono, ME 04469, USA.

[#] These authors contributed equally.

[*] Correspondence to:

James N. Sleigh j.sleigh@ucl.ac.uk Tel: +44(0)20 3448 4334

Fax: +44(0)20 7813 3107

Giampietro Schiavo giampietro.schiavo@ucl.ac.uk Tel: +44(0)20 3448 4334

Supplementary Materials and Methods

Animals

Gars$^{C201R/+}$ and *Gars*$^{Nmf249/+}$ mice were maintained as heterozygote breeding pairs on a predominantly C57BL/6 background as detailed previously (1-3). Ear clips were used for DNA extractions as formerly described (4), and animals genotyped using published protocols (1-3). Mice sacrificed for one month and three month time points were 28-36 and 88-97 days old, respectively. Post-natal day 1 (P1) was designated as the day after a litter was first found.

DRG dissection and culturing

Ethanol-sterilised 12 mm coverslips (VWR International, Radnor, PA, MENZCB00120RAC20) placed in 24-well plates (Corning, New York, NY, 3524) were treated with 20 μg/ml poly-D-lysine (Becton Dickinson, Franklin Lakes, NJ, 354210) in Ca^{2+}/Mg^{2+}-free Hank's Balanced Salt Solution (HBSS, Thermo Fisher, Waltham, MA, 14170) for at least 12 h at 4°C. Wells were washed three times with Ca^{2+}/Mg^{2+}-free Dulbecco's phosphate buffered saline (DPBS, Thermo Fisher, 14190), and thoroughly dried. 10-20 μl HBSS containing 20 μg/ml laminin (Sigma Aldrich, St. Louis, MO, L2020) was pipetted onto the centre of coverslips to concentrate the neurons and incubated at 37°C for 4-6 h. DPBS was pipetted between wells to restrict evaporation of the laminin solution. DRG neurons used in calcium imaging experiments were plated in 8-well μ-slides (Ibidi, Martinsried, Germany, 80826) treated as above, but without coverslips. Before starting the dissection, a previously prepared and frozen collagenase/dispase enzyme solution was thawed at 37°C for no longer than 2 h before use; 24 mg collagenase type II (1 U/μl, Worthington Biochemical Corporation,

Lakewood, NJ, 4176 or Thermo Fisher, 17101015) and 28 mg dispase II (Sigma, D4693) were added to 6 ml Ca^{2+}/Mg^{2+}-free HBSS, and filter-sterilised through a 0.22 μm filter (Appleton Woods, Birmingham, UK, FC121) before aliquotting and freezing. DRG were dissected as previously described (5). To limit technical variability, 20-24 DRG per animal were dissected from thoracic (T1-T13) and lumbar (L1-L5) spinal cord regions of one wild-type and one *Gars*$^{C201R/+}$ mouse during the same culturing session. DRG were enzymatically digested at 37°C for 10 min in collagenase/dispase, before manual dissociation in cell medium using a series of fire-polished glass Pasteur pipettes (VWR, 612-1701) of descending bore size. Cells were spun down at 1,000 × *g* for 5 min, before resuspension. The laminin solution was pipetted off the coverslips/μ-slides and a small volume of cells immediately added, with genotypes plated at similar densities. Cells were kept at 37°C in a 5% (v/v) CO_2 humidified atmosphere. After 1-2 h, plate and μ-slide wells were flooded with media to a total volume of 500 μl and 200 μl, respectively. F12 media + L-glutamine (Thermo Fisher, 11765) was supplemented with 10% (v/v) foetal bovine serum (FBS, Thermo Fisher, 10270), 1% (v/v) penicillin-streptomycin (10,000 U/mL, Thermo Fisher, 15140), and freshly added 20 ng/ml mouse glial cell line-derived neurotrophic factor (GDNF, Peprotech, Rocky Hill, NJ, 450-44) with 2 mg/ml bovine serum albumin (BSA, Sigma, 10735094001) in water. For calcium imaging experiments, cultures were also supplemented with 50 ng/ml mouse nerve growth factor *β* (NGF, Peprotech, 450-34) with 2 mg/ml BSA in water.

Cell immunofluorescence

All cell and tissue immunofluorescence steps were completed at room temperature, apart from overnight incubations, which were conducted at 4°C. For cell immunohistochemistry, media was carefully aspirated 24 ± 1 h post-plating, and cells

fixed with 4% (w/v) paraformaldehyde (PFA, Electron Microscopy Sciences, Hatfield, PA) for 20 min; 16% PFA stock was diluted in phosphate buffered saline (PBS, 137 mM NaCl [Sigma, S3014], 10 mM Na_2HPO_4 [Sigma, S3264], 2.7 mM KCl [Sigma, P9541], 1.8 mM KH_2PO_4 [Sigma, P9791]) to achieve the final working solution. Cells were permeabilised for 30 min using 0.3% (w/v) Triton X-100 (Sigma, T8787) in PBS, before blocking for 30 min in permeabilisation solution containing 5% (w/v) BSA, and probing overnight with primary antibodies (see below) in block solution. Triton X-100 was omitted in the non-permeabilisation protocol. The following day, coverslips were washed three times for 10 min in PBS, probed with secondary antibodies (see below) and 4',6-diamidino-2-phenylindole, dihydrochloride (DAPI, Thermo Fisher, D1306) for 2 h, and washed three times with PBS, before mounting on slides in fluorescence mounting medium (Dako, Glostrup, Denmark, S3023). Slides were kept at 4°C and allowed to set overnight before imaging.

Tissue processing for immunofluorescence

L1-L5 DRG were dissected and fixed in 4% PFA for 2 h, before washing in PBS, and equilibrating in 20% (w/v) sucrose (Sigma, S7903) in PBS overnight. Plantar punches were collected from the right hind paw using a 5 mm punch (Sigma, Z708771), fixed in 4% PFA overnight, placed in decalcifying solution (15% sucrose, 10% [w/v] ethylenediaminetetraacetic acid [EDTA, Sigma, ED2SS], 0.07% [w/v] glycerol [Sigma, G5516] in PBS) overnight, and treated with 20% sucrose in PBS overnight (6). Soleus muscles and spinal cords were dissected from mice transcardially perfused with 4% PFA at a rate of ≈3 ml/min for 4-5 min. Soleus muscles were post-fixed for 2 h, before washing with PBS and leaving in 20% sucrose overnight (7). Spinal cords were post-fixed overnight, washed with PBS, and placed in 20% sucrose overnight. The

embryonic day 18.5 (E18.5) *Kidins220*$^{-/-}$ brain (8), used as a positive control for activated caspase 3 staining (Fig. S3), was dissected in PBS, fixed for 2 h in 4% PFA, washed in PBS, and equilibrated in 20% sucrose in PBS overnight. All sucrose-treated tissues were embedded in Tissue-Tek O.C.T. Compound (Sakura Finetek, Torrance, CA, 4583), frozen on dry ice-chilled methanol (Sigma, 32213), and kept at -80°C. 10 µm DRG, one and three month plantar punch, and E18.5 brain sections, 12 µm soleus muscle sections, 20 µm P1 plantar punch sections, and 30 µm spinal cord sections were cut with an OTF Cryostat (Bright Instruments, Huntingdon, UK) and collected on polysine-coated slides (VWR, 631-0107). Transverse sections were cut from all tissues, except for the E18.5 *Kidins220*$^{-/-}$ brain (coronal), and the DRG, which were sectioned in stochastic orientations due to their spherical nature. Spinal cords were sectioned onto 12 parallel slides, L1-L5 DRG and the E18.5 brain onto eight parallel slides, soleus muscles and plantar punches on to four parallel slides, and all L5 DRG sections for neuron cell counts were collected onto 1-2 slides/DRG. All sections were air dried for 30-60 min before staining or freezing at -80°C, except for spinal cord sections, which were air dried overnight.

Tissue immunofluorescence

Sections were encircled with a hydrophobic barrier pen (Dako, S2002) on microscope slides, permeabilised by three 10 min washes with 0.3% Triton X-100 in PBS, and blocked for 1 h in 10% BSA and 0.3% Triton X-100 in PBS. To facilitate synaptic labelling, spinal cord sections were incubated for 30 min in 50% (v/v) ethanol in water, followed by 10 min in hot (>95°C) citrate-EDTA buffer (10 mM citric acid [Sigma, W302600], 2 mM EDTA, final pH 6.2 - adjusted with 10 M NaOH [Sigma, 72068]), 10 min in 4 µg/ml Proteinase K (Merck Millipore, Billerica, MA, 124568) in PBS

containing 0.3% Triton X-100, and 10 min in 1 mg/ml pepsin (Dako, S3002) in 0.2 M HCl (Sigma, 258148) at 37°C. Samples were then probed overnight with primary antibodies (see below). The following day, sections were processed in the same way as primary DRG neuron coverslips (see above), bathed in fluorescence mounting medium, and covered with 22 × 50 mm cover glass (VWR, 631-0137). E13.5 hind feet were removed from embryos between the ankle and knee joints and processed, with subtle modifications, as previously described (9). Briefly, feet were fixed for 4 h in 4% PFA, followed by overnight bleaching in 15% hydrogen peroxide (Sigma, H1009) and 1.5% dimethyl sulphoxide (DMSO, Sigma, D1435) in methanol. The following day, feet were moved to 10% (v/v) DMSO in methanol overnight, before application of primary antibody (see below) in block solution (5% normal goat serum [Sigma, G9023] and 20% DMSO in PBS) for five days. Feet were subsequently washed five times in PBS for 1 h, before applying secondary antibody in block overnight. Finally, feet were washed three times in PBS for 1 h before mounting on microscope slides in Dako medium, and covering with 22 × 50 mm cover glass.

Antibodies for immunohistochemistry

The following primary antibodies were used (Tables S1-2) for immunofluorescence and western blotting: sheep anti-calcitonin gene-related peptide (CGRP, Enzo Life Sciences, Farmingdale, NY, BML-CA1137), goat anti-choline acetyltransferase (ChAT, Merck Millipore, AB144P), rabbit anti-cleaved-caspase 3 (Cell Signaling Technology, Danvers, MA, 9661), rabbit anti-extracellular signal-regulated kinases 1 and 2 (ERK1/2, Cell Signaling Technology, 9102), rabbit anti-p-ERK1/2 (Cell Signaling Technology, 9101), mouse anti-FLAG (Sigma, F1804), mouse anti-glyceraldehyde-3-phosphate dehydrogenase (GAPDH, Merck Millipore, MAB374),

rabbit anti-laminin (Sigma, L9393), rabbit anti-NeuN (Abcam, Cambridge, UK, ab177487), mouse anti-neurofilament (2H3, developed by Thomas M. Jessell and Jane Dodd, Developmental Studies Hybridoma Bank, Iowa City, IA, supernatant), mouse anti-NF200 (Sigma, N0142), rabbit anti-parvalbumin (Swant, Marly, Switzerland, PV27), rabbit anti-peripherin (Merck Millipore, AB1530), rabbit anti-PGP9.5 (UltraClone, Isle of White, UK, 31A3), rabbit anti-PSD95 (Frontier Institute, Ishikari, Japan, Af628), mouse pan anti-synaptic vesicle 2 (SV2, developed by Kathleen M. Buckley, Developmental Studies Hybridoma Bank, Iowa City, IA, concentrate), guinea pig anti-synaptophysin (Frontier Institute, Af300), rabbit anti-TrkB (Merck Millipore, 07-225), rabbit anti-TRPV1 (Alomone Labs, Jerusalem, Israel, ACC-030), chicken anti-βIII-tubulin (Abcam, ab41489), mouse anti-βIII-tubulin (Covance, Princeton, NJ, mms-435P), and mouse anti-V5 (Invitrogen, Carlsbad, CA, R960CUS). For immunofluorescence, tissues were also sometimes incubated with 1 mg/ml isolectin B_4 (IB4) biotin conjugate from *Bandeiraea simplicifolia* (Sigma, L2140) in PBS at 1/250. The following day, combinations of AlexaFluor secondary antibodies (Thermo Fisher, A-10040, A-11001, A-11008, A-11034, A-11039, A-11055, A-11074, A-21235, A-21236, A-21245, A-21424, A-21429, A-21436) at 1/1,000, 2 mg/ml streptavidin, Pacific Blue conjugate (Thermo Fisher, S-11222) or streptavidin, AlexaFluor 488 conjugate (Thermo Fisher, S-11223) at 1/250, and DAPI at 1/1,000 in PBS were used.

Cell imaging and analysis

Mounted cells were imaged using an Axioplan 2 microscope (Zeiss, Oberkochen, Germany) or a LSM 780 laser scanning microscope (Zeiss), and single plane images analysed using ImageJ software (https://imagej.nih.gov/ij/). Cell bodies and processes of DRG neurons were visualised using the pan-neuronal marker βIII-tubulin. To

calculate the percentage of cells bearing neurites an average of 788 cells/coverslip were scored. Neuronal processes shorter than approximately half of the diameter of the cell body of the largest neurons (≈15 μm), as assessed by eye, were not counted as neurites. Neurite lengths were measured by manually plotting points along the length of a cell's longest process, and an average of 51 cells/coverslip were assessed. Cell body area was measured by manually drawing around the circumference of the cell body, and an average of 202 cells/coverslip were assessed. To assess activated caspase 3 staining, the average fluorescence intensity of βIII-tubulin$^+$ cell bodies was calculated for each coverslip, and the mean cell body fluorescence from the secondary only control was subtracted. DRG neurons were plated onto multiple coverslips, which were then PFA-fixed at different times post-plating (4, 48, and 96 h). Coverslips were simultaneously processed, and images acquired with the same confocal settings, so that fluorescence intensity could be compared across time points. An average of 57 cells/coverslip were assessed for cleaved-caspase 3 intensity. To categorise neurons, cells were divided into small (<315 μm^2), medium (315-706 μm^2), and large (>706 μm^2) groups based on previously published criteria (10), and an average of 202 cells/coverslip were assessed. To assess the percentage of βIII-tubulin$^+$ cells expressing NF200, an average of 241 cells/coverslip were scored by eye. All DRG culture analyses include multiple coverslips (1-3)/animal and were performed blinded to genotype.

Tissue imaging and analysis

All mounted tissues, except for spinal cord sections, were imaged using a LSM 780 laser scanning microscope (Zeiss), and images analysed using ImageJ software. Spinal cord sections were imaged with a LSM 710 laser scanning microscope (Zeiss). To measure the area of βIII-tubulin$^+$ profiles in L1-L5 DRG sections, z-stack images were

taken with a 20x objective, and 3D projected (Max Intensity) images used to draw around the circumference of cell profiles. The areas of 300 profiles/DRG were averaged from three DRG to generate a single mean value for each mouse. Single plane, tile scan images of L1-L5 DRG sections were taken with a 10x or 20x objective to calculate the percentages of $CGRP^+$, $IB4^+$, $NF200^+$, $peripherin^+$, and $parvalbumin^+$ cells, and measure average TRPV1 fluorescence intensity. The Cell Counter ImageJ plugin was used to avoid re-counting cells, and an average of 470 profiles/DRG from three DRG were scored and used to calculate a mean percentage value for each mouse. Anti-TRPV1 stained sections were converted to black and white, and inverted, before thresholding uniformly across samples in order to identify $TRPV1^+$ neurons. The Freehand Selection tool was then used to measure the average cytoplasmic fluorescence intensity per $TRPV1^+$ cell. The mean value of these TRPV1 intensities was calculated for three separate DRG. The average of the three mean values was calculated, and the mean background fluorescence level from secondary only control slides subtracted to produce a value for each animal. An average of 15 cells/DRG section were analysed. Activated caspase 3 levels were assessed by measuring the average fluorescence intensity of each DRG section, and subtracting from this value the fluorescence of secondary-only control sections. All slides within a time point (i.e. P1, one, and three months) were processed in parallel and images acquired in the same session with identical settings. Three sections/DRG were used to produce a mean value for each DRG, which was then averaged across three DRG to get a cleaved-caspase 3 fluorescence intensity for each mouse. To perform βIII-$tubulin^+$ profile counts in L5 DRG, the volume of each DRG (in mm^3) was estimated by calculating the mean area (in mm^2) of 15-17 evenly-spaced sections and then multiplying this value by the thickness and number of sections taken for each DRG (71-116). The number of βIII-

tubulin^{+} profiles was counted in each of the sections and averaged to get an estimate of neuron density (neurons/mm^{3}). DRG volume and neuron density values were then used to estimate the number of profiles/L5 DRG. For soleus muscle spindle analyses, a full series of sections across the length of each muscle was used to count the number of spindles. Muscle spindles were identified based on SV2/2H3 fluorescence and, because this antibody combination is also used to visualise NMJs (11), stereotypical architecture. Spindle innervation status was assessed by eye by scoring the percentage of spindles displaying the characteristic circular SV2/2H3 fluorescence surrounding central, large circular nuclei (e.g. Fig. 3A, wild-type). Spindles lacking this staining around at least one nuclei were designated as not fully innervated (e.g. Fig. 3A, *Gars*$^{C201R/+}$). All spindles within each muscle were assessed. To analyse intraepidermal nerve fibre density, z-stack images of the epidermis were taken of the central region of the lateral edge of glabrous hind paw using a 20x objective. Images were 3D projected (Max Intensity), uniformly thresholded across samples (PGP9.5 staining assigned to black and background to white), and all particles analysed within the epidermis. The summed pixel area was then divided by the epidermis area to get percentage coverage of PGP9.5 staining/10 μm section. This value was halved for P1 samples, which were sectioned at twice the thickness of the one and three month plantar punches. Samples within time points were simultaneously processed and imaged with identical microscope settings. Six to eight sections were used to generate mean values for each animal, and secondary only control slides were used to ensure that background fluorescence did not impact the final result. To assess E13.5 sensory nerve targeting of the hind limbs, single-plane, tile scan images were taken with a 20x objective. Images were then used to measure the distances between the ventral and dorsal main nerve trunk endings to the tips of the developing digits. The average distance of 2-6 nerves

was calculated to produce values for each embryo. Nerve branching in the dorsal foot plate was also assessed by calculating the number of branches per mm of the longest length of each major nerve trunk and then averaging those values to produce a score for each embryo, similar to previously reported (12). In order to prevent subtle differences in developmental stage impacting the result, statistical analyses at E13.5 were performed not on raw data but values relative to the wild-type mean. For spinal cord synaptic content, three sections were assessed per animal, and for the motor neuron analysis, four ventral horns were imaged per animal. All images were captured with a voxel size of 40 × 40 nm by 100 nm depth using a x63 Plan-Apochromat objective. To analyses synapse numbers, a single image slice (≈75 μm width × 150 μm height) of IB4 and PSD95 labelling was initially taken across one randomly selected superficial dorsal horn, including laminae I-III, from the tissue section under analysis. Using the freehand drawing tool and ROI (Region of Interest) Manager in ImageJ and IB4 labelling as a marker of lamina II, this reference image was used to delineate regions of interest consisting of lamina I, II outer, II inner, and III. These regions of interest were used for assessing synapse densities across the different laminae of the dorsal horn. Sample image stacks were also captured of the same region, taken to a depth of 5.5 μm, and processed to derive binary representations of synaptic puncta. Firstly, stacks were deconvolved in ImageJ using the WPL deconvolution algorithm in the Parallel Iterative Deconvolution software package (13), based on the Iterative Deconvolve 3D plugin (14). 3D PSFs were generated in PSF Lab (15). Deconvolved image stacks were then filtered with the "despeckle" 3 × 3 median filter and thresholded using the OTSU method in ImageJ. To assess puncta within each region of interest, the image stack was divided into eight equally spaced image slices (0.1 μm z slices separated by 0.5 μm). Each region on the isolated slices was assessed separately for $PSD95^{+}$ and

synaptophysin^{+} puncta profiles using the Analyze Particles plugin in ImageJ. Puncta profile counts for each lamina were averaged across three tissue sections per animal, and plotted as puncta profile numbers per 100 μm^2 of lamina. To assess motor neuron subtype proportions, z-stack images of the entire section depth were maximally projected, the border of the lateral-medial nucleus of lamina IX delineated, and the number of ChAT^{+}, NeuN^{+}, and ChAT^{+}/NeuN^{+} neurons quantified. From this data, the number of alpha (ChAT^{+}/NeuN^{+}) and gamma (ChAT^{+}/NeuN^{-}) neurons were calculated as a proportion of total neurons. All phenotypic analyses in this study were performed blinded to genotype.

Sensory behaviour testing

For all sensory behaviour tests, mice were pre-acclimatised to the testing equipment and an average of 2-3 baseline readings were used to obtain a final measurement. To assess mechanosensation, von Frey monofilaments were applied to the plantar surface of the hind paw and removal of the paw recorded as a positive response. A response threshold value was calculated using the up and down method (16). Proprioception was assessed using the beam walk test as previously described (17). Briefly, mice were filmed as they moved across a thin wooden beam of roughly one meter in length. The percentage of correct steps was calculated by recording the number of missed hind paw placements and hops, and comparing to the total number of steps taken for each run. Noxious mechanical thresholds were calculated with the use of an Analgesy-Meter (Ugo Basile, 37215) (18). Mice were lightly restrained and increasing mechanical pressure was applied either to the dorsum of the paw or to the base of the tail. The force at which an obvious withdrawal response was observed was taken as the withdrawal threshold. To assess heat sensitivity, the Hargreaves method was used (19). A radiant

heat source was applied to the plantar surface of the hind paw and the latency to withdrawal was measured as the noxious heat threshold. All tests were carried out with the experimenter blind to genotype.

Motor behaviour testing

Motor behaviour was assessed using a Grip Strength Meter (Bioseb, Vitrolles, France, GS3) and an accelerating Rota-Rod (Ugo Basile, Monvalle, Italy, 47600) as previously described (2, 20). Rota-Rod testing was sometimes performed before grip strength testing on the same day with at least a 30 min interval between tests. Mice were tested on two or three days within a week. Three trials were performed per animal per test day, with at least 5 min rest between trials. The maximum recorded value from the three trials in a day was used to calculate a mean value across days for each mouse.

Measurement and analysis of cytosolic calcium

Cytosolic calcium in primary DRG neurons was assessed as previously described (21). Briefly, cells were washed twice with recording medium (156 mM NaCl, 10 mM D-glucose [Sigma, G8270], 10 mM HEPES [Sigma, H3375], 3 mM KCl [Sigma, P9333], 2 mM $CaCl_2$ [Sigma, C8106], 2 mM $MgSO_4$ [Sigma, M7506], and 1.25 mM KH_2PO_4, final pH 7.34-7.36 - adjusted with 10 M NaOH), and loaded with 5 μM fura-2 AM (Thermo Fisher, F1221) and 0.002% (v/v) pluronic acid F-127 (Thermo Fisher, P3000MP) in recording medium for 30 min at room temperature. Fura-2 was subsequently removed and cells washed twice in recording medium before cytosolic calcium was detected in single cells every 2 s using an IX70 inverted microscope (Olympus, Tokyo, Japan), a cooled Retiga Fast 1394 CCD camera (QImaging, Surrey, Canada), and Andor iQ 1.9 software (Belfast, UK). Following at least 90 s continuous

recording of the baseline fura-2 ratio, the medium was carefully replaced with recording medium containing either 50 mM KCl or 1 μM capsaicin (Sigma, M2028). To calculate the fura-2 ratio change from baseline to maximal response for individual cells, the mean of 20 sequential recordings post-stimulation was divided by the mean of 20 sequential baseline recordings prior to stimulation. The mean average was then calculated for all cells simultaneously imaged in a well. An average of 10 cells per well was assessed. Capsaicin responsive and non-responsive cells were categorised based on whether the percentage fura-2 ratio change was ≥ 150% or < 150%, respectively. Fura-2 experiments include multiple wells (2-3)/treatment/animal.

Cell culture and transfection

NSC-34 and N2a neuroblastoma cells stably transfected with human TrkB N-terminally tagged with FLAG (22) were grown in Dulbecco's Modified Eagle Medium (DMEM, Thermo Fisher, 41966) supplemented with 10% FBS (Omega Scientific, Singapore or Thermo Fisher), and 1% penicillin-streptomycin. N2a media was also supplemented with 1% (v/v) GlutaMAX (Thermo Fisher, 35050061). Cells were maintained at 37°C in a 5% CO_2 humidified atmosphere and split every 2-3 days using 0.25% (v/v) trypsin-EDTA (Thermo Fisher, 25200). For immunofluorescence, N2a cells were plated onto PDL-treated coverslips at 2.5×10^5 cells/well and left overnight before processing (as outlined above). NSC-34 cells were grown to ≈70% confluency and transfected with pcDNA6 plasmids expressing human wild-type, P234KY, or C157R *GARS* with a C-terminal V5 tag using Lipofectamine 2000 (Invitrogen, 116680) according to manufacturer's instructions.

Protein extraction

L1-L5 DRG were dissected from one month old, PBS-perfused (see above) mice, and collected into microcentrifuge tubes containing PBS, which were spun down to pellet the ganglia and remove the PBS, before snap freezing in liquid nitrogen. Samples were subsequently thawed on ice, and ground up with a plastic mortar and pestle (VWR, 431-0094) in RIPA lysis buffer (150 mM NaCl, 50 mM Tris-HCl [Sigma, T3253, pH 7.5], 1% [w/v] sodium deoxycholate [Sigma, D6750], 1% Triton X-100, 0.1% [w/v] sodium dodecyl sulphate [Sigma, L3771]), and left for 30 min on ice, before clearing for 20 min at 10,000 × *g*. For pull-down experiments, 36 h post-transfection NSC-34 cells were twice washed in PBS, collected in microcentrifuge tubes, pelleted, and re-suspended in Pierce IP Lysis Buffer (Thermo Fisher, 87787) for 30 min, and the extract cleared for 7 min at 12,000 × g. Protein was extracted from N2a cells in a similar manner using NP-40 lysis buffer (150 mM NaCl, 10 mM Tris-HCl [pH 8.0], 1% IGEPAL CA-630 [Sigma, I3021], 1 mM EDTA). Halt protease and phosphatase inhibitor cocktail (Thermo Scientific, 78445) was freshly added to RIPA and NP-40 lysis buffers.

In vitro pull-down assay

Recombinant human TrkA (R&D Systems, Minneapolis, MN #175-TK), TrkB (R&D Systems, #688-TK), and TrkC (R&D Systems, #373-TC/CF) Fc chimeras were bound to Protein G beads (Invitrogen). NSC-34 cell extracts containing the V5-tagged WT, P234KY, or C157R GlyRS were individually added to the receptor-immobilised beads and incubated for 1 h at 4°C. The beads were then washed three times with buffer (100 mM NaCl, 50 mM Tris-HCl [pH 7.5], 5% glycerol, 0.1% Triton X-100), and the immunoprecipitates probed by western blot analysis against the V5 tag.

Western blotting

Immunoprecipitates and protein lysates were fractionated by 4-12% or 4-15% (v/v) Bis-Tris-Plus SDS-PAGE gels (Invitrogen or Bio-Rad, Hercules, CA) and transferred to PVDF membranes using the iBlot Dry Blotting System (Invitrogen) or Trans-Blot Turbo Transfer System (Bio-Rad). Membranes were blocked for 1 h with Tris-buffered saline containing 0.1% (v/v) Tween 20 (Sigma, P2287) and 5% (w/v) non-fat dry milk or 5% BSA (for anti-phospho antibodies), before exposure to primary antibodies in blocking solution overnight (see above). The following day, membranes were washed and probed with HRP-conjugated anti-mouse or anti-rabbit secondary antibodies (Cell Signaling Technology or Dako), followed by detection using ECL western blotting substrate (Thermo Fisher Scientific or Merck Millipore) and exposure using the ChemiDoc Touch Imaging System (Bio-Rad). Densitometry analysis was performed as described previously (4). ERK1/2 phosphorylation levels were compared by running the same lysates in two parallel gels, and probing one for total ERK1/2 and the other for p-ERK1/2.

Trk activation assays

N2a cells were plated in 2 ml media in 6-well plates at $1.5x10^6$ cells/well, and serum-starved 3 h later for 3 h by replacing the media with DMEM lacking FBS. The cell media was then aspirated and replaced with fresh media containing an equivalent volume of PBS (<1% v/v), 150 nM wild-type, L129P, or G240R GlyRS; the applied extracellular concentration of GlyRS was similar to previously published studies (23, 24). One well per plate was left untreated to assess perturbations in ERK phosphorylation caused by temporary removal from the incubator. After 5, 15, or 30 min incubations, cells were placed on ice, lysed, and analysed by western blot as

outlined above and described recently elsewhere (22). Recombinant GlyRS proteins were produced as previously described (24).

Supplementary References

1. Seburn KL, Nangle LA, Cox GA, Schimmel P, & Burgess RW (2006) An active dominant mutation of glycyl-tRNA synthetase causes neuropathy in a Charcot-Marie-Tooth 2D mouse model. *Neuron* 51(6):715-726.
2. Achilli F, *et al.* (2009) An ENU-induced mutation in mouse glycyl-tRNA synthetase (*GARS*) causes peripheral sensory and motor phenotypes creating a

model of Charcot-Marie-Tooth type 2D peripheral neuropathy. *Dis Model Mech* 2(7-8):359-373.

3. Stum M, *et al.* (2010) An assessment of mechanisms underlying peripheral axonal degeneration caused by aminoacyl-tRNA synthetase mutations. *Mol Cell Neurosci* 46(2):432-443.
4. Sleigh JN, *et al.* (2014) Chondrolectin affects cell survival and neuronal outgrowth in *in vitro* and *in vivo* models of spinal muscular atrophy. *Hum Mol Genet* 23(4):855-869.
5. Sleigh JN, Weir GA, & Schiavo G (2016) A simple, step-by-step dissection protocol for the rapid isolation of mouse dorsal root ganglia. *BMC Res Notes* 9(1):82.
6. Shepherd AJ & Mohapatra DP (2012) Tissue preparation and immunostaining of mouse sensory nerve fibers innervating skin and limb bones. *J Vis Exp* (59):e3485.
7. Oliveira Fernandes M & Tourtellotte WG (2015) Egr3-dependent muscle spindle stretch receptor intrafusal muscle fiber differentiation and fusimotor innervation homeostasis. *J Neurosci* 35(14):5566-5578.
8. Cesca F, *et al.* (2012) Kidins220/ARMS mediates the integration of the neurotrophin and VEGF pathways in the vascular and nervous systems. *Cell Death Differ* 19(2):194-208.
9. Wickramasinghe SR, *et al.* (2008) Serum response factor mediates NGF-dependent target innervation by embryonic DRG sensory neurons. *Neuron* 58(4):532-545.

10. Sommer EW, Kazimierczak J, & Droz B (1985) Neuronal subpopulations in the dorsal root ganglion of the mouse as characterized by combination of ultrastructural and cytochemical features. *Brain Res* 346(2):310-326.
11. Sleigh JN, Burgess RW, Gillingwater TH, & Cader MZ (2014) Morphological analysis of neuromuscular junction development and degeneration in rodent lumbrical muscles. *J Neurosci Methods* 227:159-165.
12. Vieira JM, Schwarz Q, & Ruhrberg C (2007) Selective requirements for NRP1 ligands during neurovascular patterning. *Development* 134(10):1833-1843.
13. Wendykier P & Nagy JG (2010) Parallel Colt: A high-performance Java library for scientific computing and image processing. *Acm T Math Software* 37(3).
14. Dougherty R (2005) Extensions of DAMAS and benefits and limitations of deconvolution in beamforming. *11th AIAA/CEAS Aeroacoustics Conferences, Monterey, California.*
15. Nasse MJ & Woehl JC (2010) Realistic modeling of the illumination point spread function in confocal scanning optical microscopy. *J Opt Soc Am A Opt Image Sci Vis* 27(2):295-302.
16. Chaplan SR, Bach FW, Pogrel JW, Chung JM, & Yaksh TL (1994) Quantitative assessment of tactile allodynia in the rat paw. *J Neurosci Methods* 53(1):55-63.
17. Carter RJ, Morton J, & Dunnett SB (2001) Motor coordination and balance in rodents. *Current Protoc Neurosci / editorial board, Crawley JN, et al.* Chapter 8, Unit 8 12.
18. Randall LO & Selitto JJ (1957) A method for measurement of analgesic activity on inflamed tissue. *Arch Int Pharmacodyn Ther* 111(4):409-419.

19. Hargreaves K, Dubner R, Brown F, Flores C, & Joris J (1988) A new and sensitive method for measuring thermal nociception in cutaneous hyperalgesia. *Pain* 32(1):77-88.

20. Bogdanik LP, *et al.* (2013) Loss of the E3 ubiquitin ligase LRSAM1 sensitizes peripheral axons to degeneration in a mouse model of Charcot-Marie-Tooth disease. *Dis Model Mech* 6(3):780-792.

21. Domijan AM, Kovac S, & Abramov AY (2014) Lipid peroxidation is essential for phospholipase C activity and the inositol-trisphosphate-related Ca^{2+} signal. *J Cell Sci* 127(Pt 1):21-26.

22. Terenzio M, *et al.* (2014) Bicaudal-D1 regulates the intracellular sorting and signalling of neurotrophin receptors. *EMBO J* 33(14):1582-1598.

23. Park MC, *et al.* (2012) Secreted human glycyl-tRNA synthetase implicated in defense against ERK-activated tumorigenesis. *Proc Natl Acad Sci U S A* 109(11):E640-647.

24. He W, *et al.* (2015) CMT2D neuropathy is linked to the neomorphic binding activity of glycyl-tRNA synthetase. *Nature* 526(7575):710-714.

Supplementary Figures

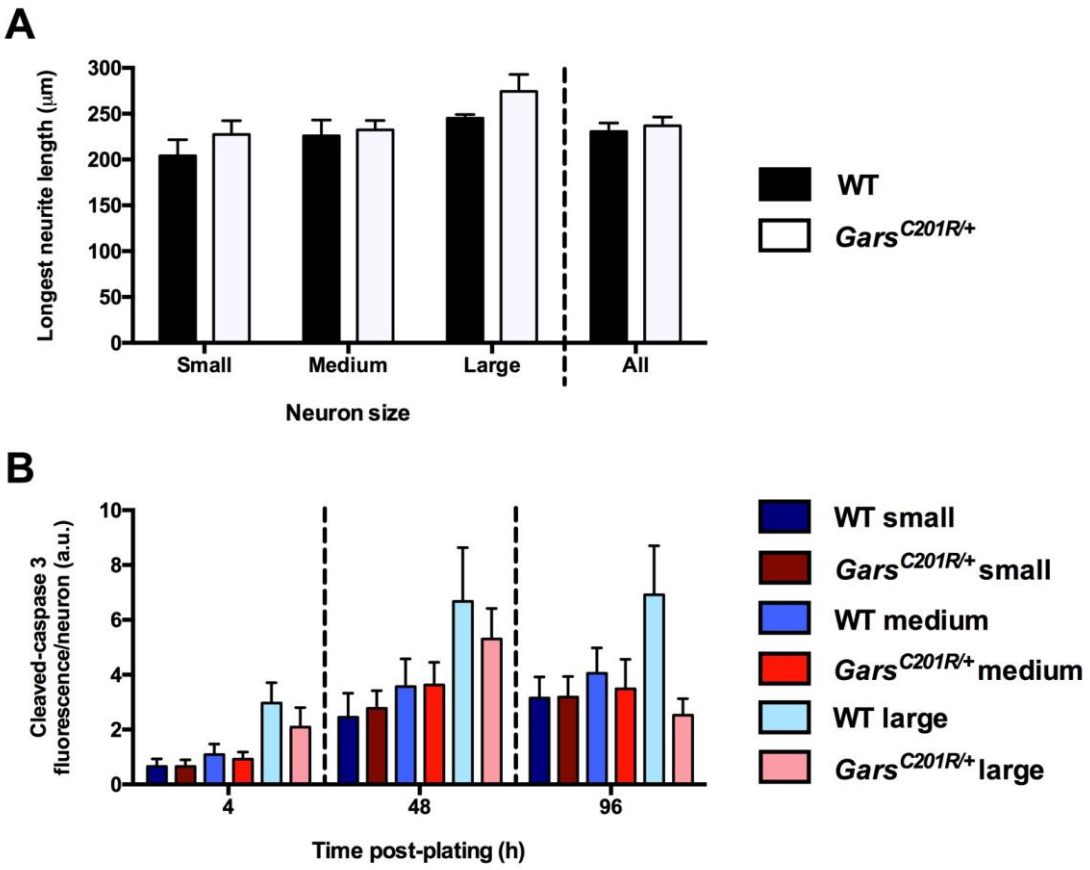

Supplementary Figure 1. Different classes of mutant sensory neuron, based on cell soma size, are equally unaffected. (**A**) Small (<315 μm^2), medium (315-706 μm^2), and large (>706 μm^2) area sensory neurons show no difference in the longest neurite length between wild-type and *Gars*$^{C201R/+}$ cultures. Neurons were stained with anti-βIII-tubulin. P = 0.05, Kruskal-Wallis test, P > 0.05, Dunn's multiple comparison tests between wild-type and mutant samples of all cell sizes (excluding "All" category, which was tested in Fig. 1A, top right). (**B**) There is also no evidence for greater cell death, as assessed by measuring activated caspase 3 fluorescence intensity per neuron. 4 h time point, P = 0.047, Kruskal-Wallis test, P > 0.05, Dunn's multiple comparison tests between wild-type and mutant samples of all cell sizes; 48 h time point, two-way ANOVA (P = 0.018, cell body size; P = 0.729, genotype; P = 0.739, interaction); 96 h

time point, two-way ANOVA (P = 0.362, cell body size; P = 0.071, genotype; P = 0.099, interaction). a.u., arbitrary units. n = 4.

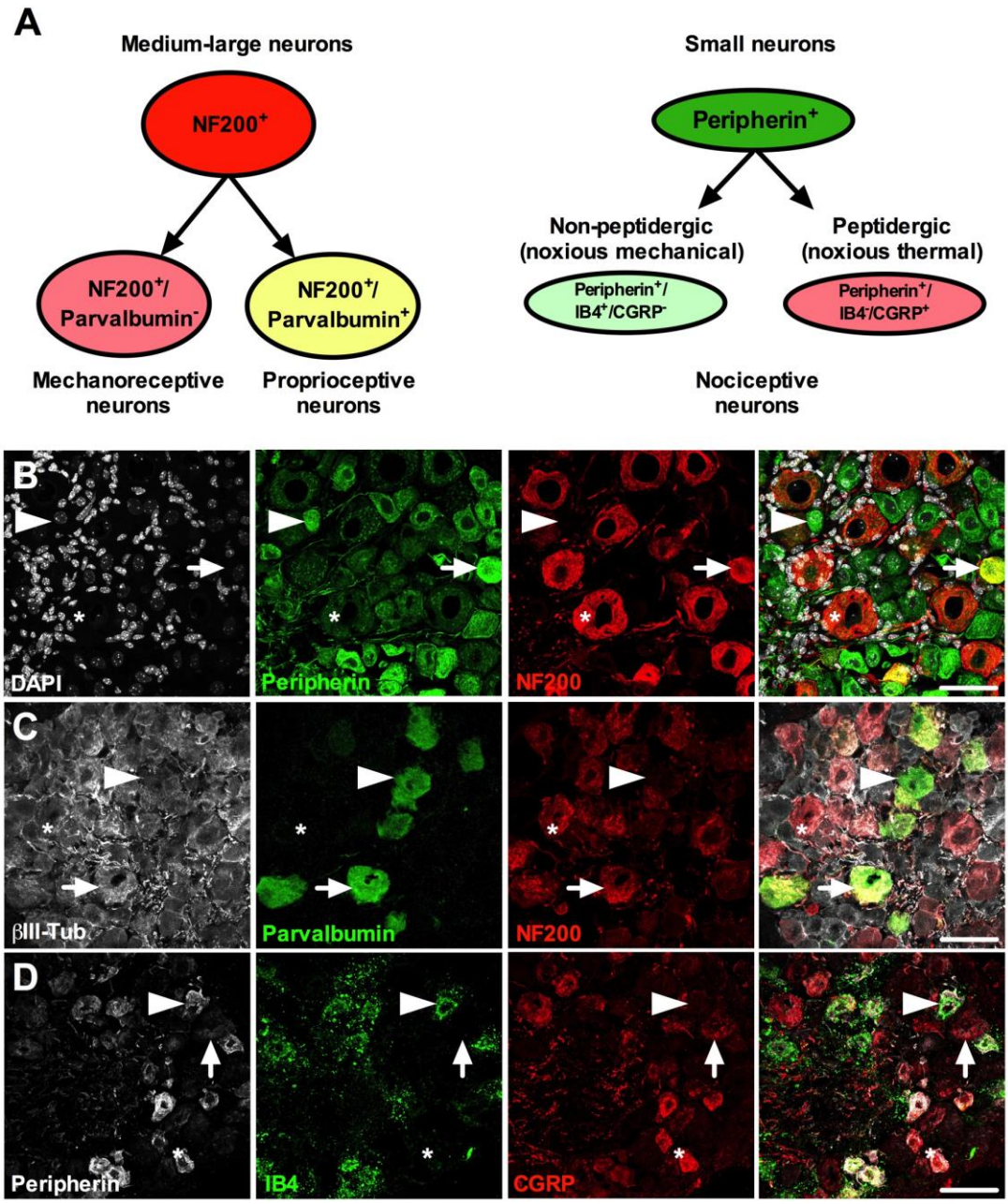

Supplementary Figure 2. Immunohistochemical analysis of functional sensory neuron subtype markers. (**A**) Different functional classes of sensory neurons can be identified based on the expression of marker proteins. NF200 and peripherin are mostly exclusively expressed in medium-large (A-fibres) and small (Aδ and C-fibres) sensory nerves, respectively. $NF200^+$ cells lacking parvalbumin expression are considered to be mechanoreceptive neurons, while those that are $parvalbumin^+$ are proprioceptive (A,

left-hand side). Peripherin^{+} cells that co-stain with isolectin B_4 (IB4), but not calcitonin gene-related peptide (CGRP), are non-peptidergic, mainly mechanical nociceptors, and those peripherin^{+} cells that are labelled with CGRP, but not IB4, are peptidergic, principally thermal, nociceptors (A, right-hand side). (**B**) Representative example of co-staining with DAPI (white), peripherin (green), and NF200 (red). The asterisk highlights a NF200^{+}/peripherin^{-} medium-large neuron, and the arrowhead marks a NF200^{-}/peripherin^{+} small neuron. The arrow identifies an infrequently seen (≈2-3%) cell type that expresses both NF200 and peripherin. A second such cell (yellow) can be seen towards the bottom of the merged image. (**C**) Representative example of co-staining with βIII-tubulin (white), parvalbumin (green), and NF200 (red). The asterisk identifies a NF200^{+}/parvalbumin^{-} cell likely to be a mechanoreceptive sensory neuron, the arrow marks a NF200^{+}/parvalbumin^{+} proprioceptive nerve, and the arrowhead highlights a rare NF200^{-}/parvalbumin^{+} cell. (**D**) Representative example of co-staining with peripherin (white), IB4 (green), and CGRP (red). The arrowhead identifies a peripherin^{+}/IB4^{+}/CGRP^{-} neuron, which is likely a mechanosensitive nociceptor, the asterisk marks a peripherin^{+}/IB4^{-}/CGRP^{+} nociceptor probably sensitive to noxious thermal stimuli, and the arrow highlights an uncommon (≈1%) example of a peripherin^{-}/IB4^{-}/CGRP^{+} cell. All images are collapsed z-stacks taken of one month wild-type DRG. Scale bars = 50 μm.

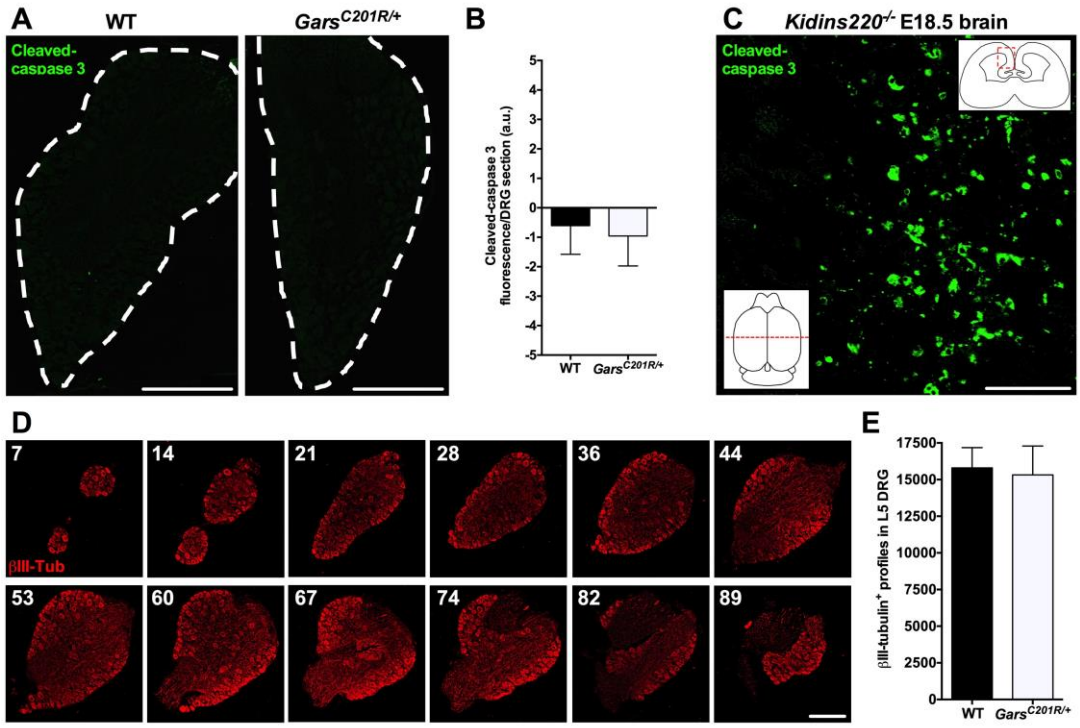

Supplementary Figure 3. *Gars*$^{C201R/+}$ DRG show no signs of sensory neuron loss at one month. (**A**) Representative single confocal plane images of one month old wild-type (left) and *Gars*$^{C201R/+}$ DRG sections stained for the apoptotic marker cleaved-caspase 3. DRG sections are outlined by dashed lines. (**B**) There is no difference in cleaved-caspase 3 fluorescence intensity between wild-type and mutant DRG. P = 0.812, unpaired t-test. a.u., arbitrary units. (**C**) Representative cleaved-caspase 3 staining of a section taken from an E18.5 *Kidins220*$^{-/-}$ brain, which was used as a positive control. Inset images depict the region of the coronal section (bottom left), and the area of the section that was imaged (top right). (**D**) Representative images of serial sections taken from a single wild-type L5 DRG and stained with βIII-tubulin (red). The number in the top left of each panel depicts the section number. Serial sections were taken throughout the entire length of the DRG in order to estimate the number of sensory neurons per L5 ganglion. (**E**) βIII-tubulin^{+} cell profile estimates indicate that *Gars*$^{C201R/+}$ L5 DRG show no signs of sensory neuron loss. P = 0.849, unpaired t-test.

n = 4. All images are single confocal planes. Scale bars = 200 μm (A, D) and 50 μm (C).

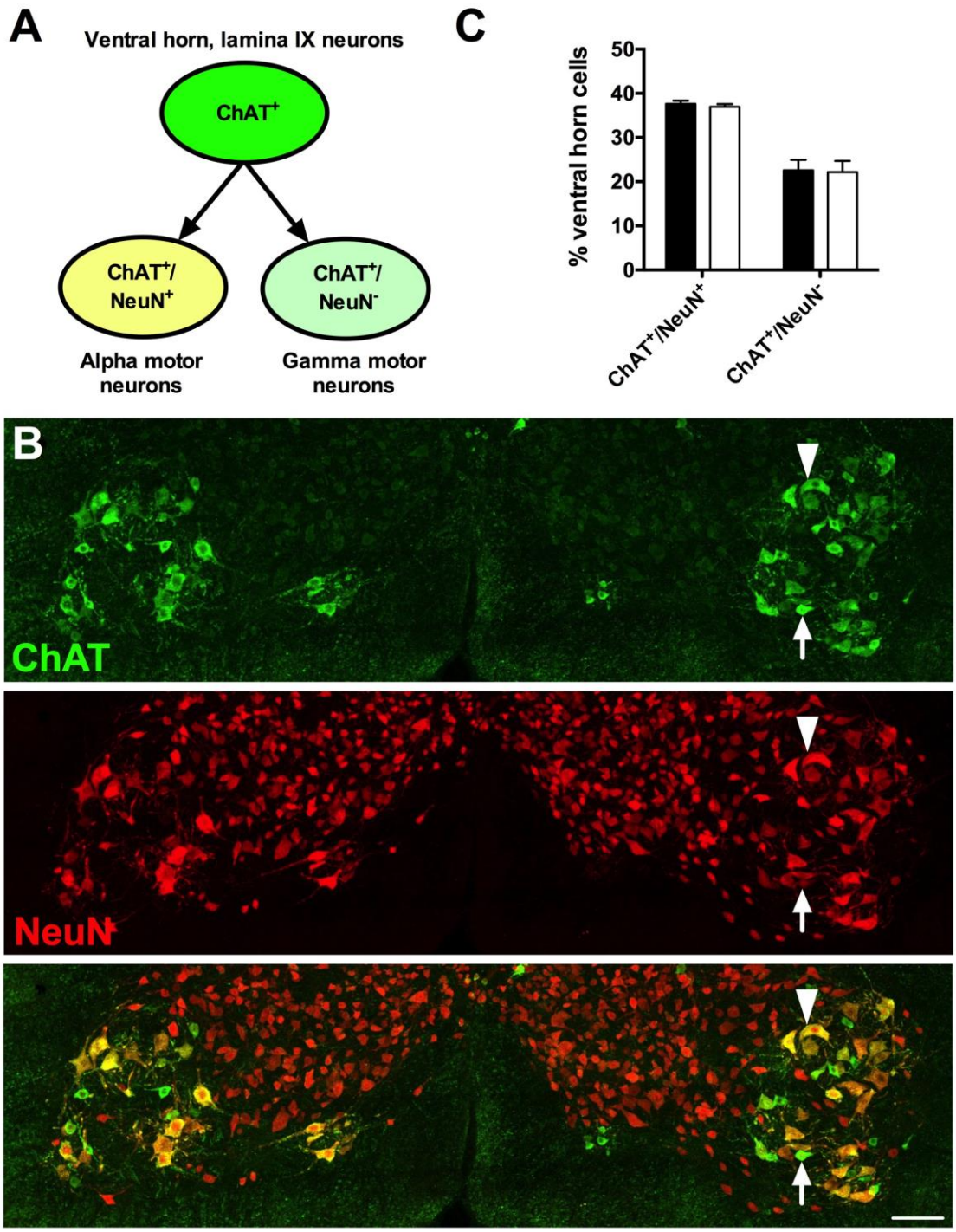

Supplementary Figure 4. The proportions of alpha and gamma spinal cord motor neurons are unaffected in *Gars*$^{C201R/+}$ mice. (**A**) The cell bodies of alpha and gamma motor neurons located in the ventral horn of the spinal cord can be differentiated by marker protein expression. Based on their size and location in lamina IX, cells

expressing choline acetyltransferase (ChAT) and NeuN are alpha motor neurons, while $ChAT^{+}/NeuN^{-}$ cells are gamma motor neurons. (**B**) Representative collapsed z-stack image of one month old wild-type spinal cord section stained for ChAT (green) and NeuN (red). Example alpha (arrowhead) and gamma (arrow) motor neurons are identified. Scale bar = 100 μm. (**C**) At one month, there is no difference between wild-type and $Gars^{C201R/+}$ mice in the proportion of alpha or gamma motor neurons found in lamina IX of the spinal cord. Two-way ANOVA ($P < 0.001$, motor neuron subtype; $P = 0.763$, genotype; $P = 0.950$, interaction). $n = 3$.

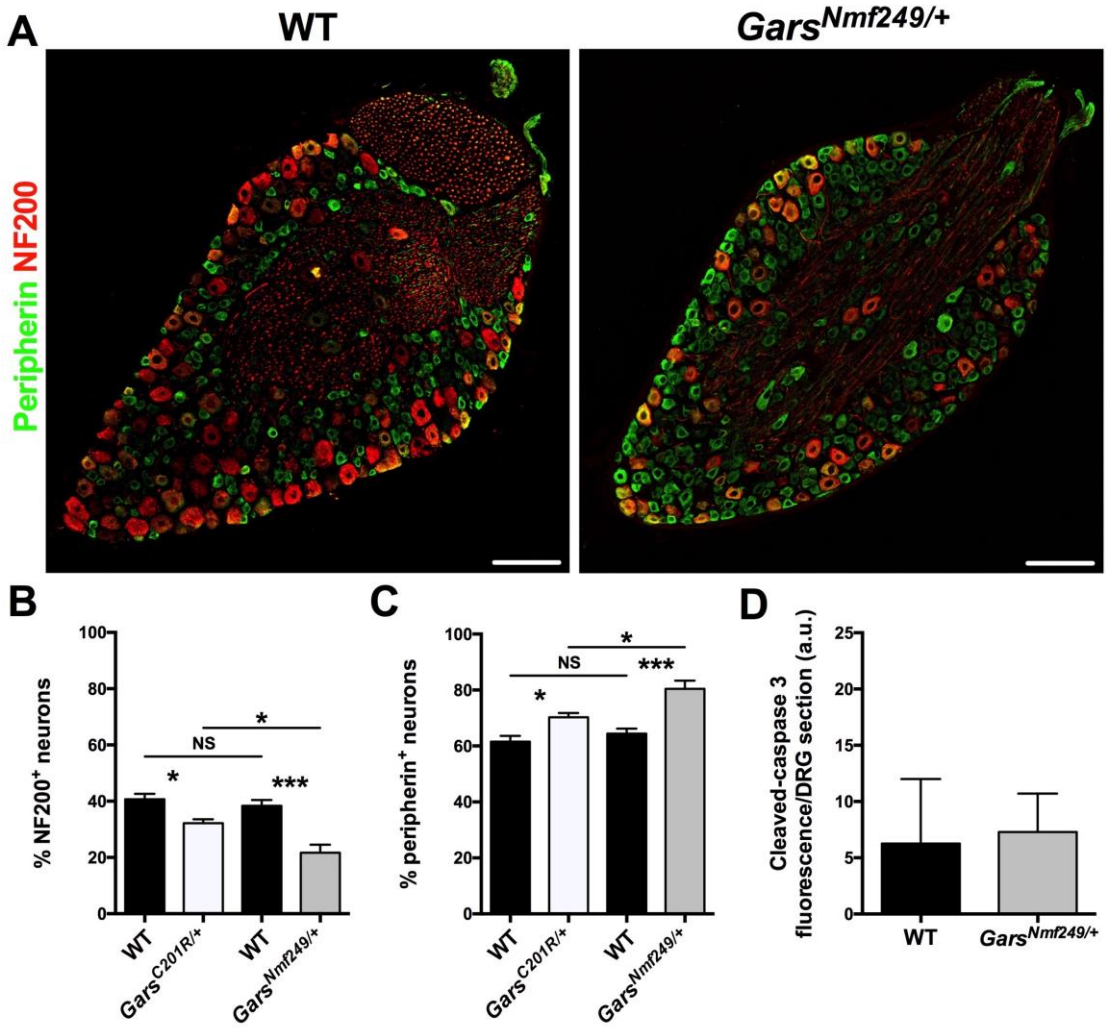

Supplementary Figure 5. *Gars* mouse DRG defects correlate with mutant severity. (**A**) Representative single confocal plane images of one month old DRG taken from wild-type (left) and the more severe CMT2D mutant mouse model, $Gars^{Nmf249/+}$, stained for peripherin (green) and NF200 (red). Scale bars = 100 μm. (**B-C**) $Gars^{Nmf249/+}$ mice display a significant reduction in the percentage of $NF200^{+}$ cells (B, $P < 0.001$, one-way ANOVA), and a concomitant increase in the percentage of $peripherin^{+}$ cells (C, $P < 0.001$, one-way ANOVA) compared to both wild-type and $Gars^{C201R/+}$ mice. NS, not significant, * $P < 0.05$, *** $P < 0.001$, Sidak's multiple comparisons test. $Gars^{C201R/+}$ data are taken from Fig. 2. (**D**) There is no evidence for increased levels of cell death

in the *Gars*$^{Nmf249/+}$ DRG, as assessed by activated caspase 3 staining. a.u., arbitrary units. $P = 0.882$, unpaired *t*-test. $n = 4\text{-}5$.

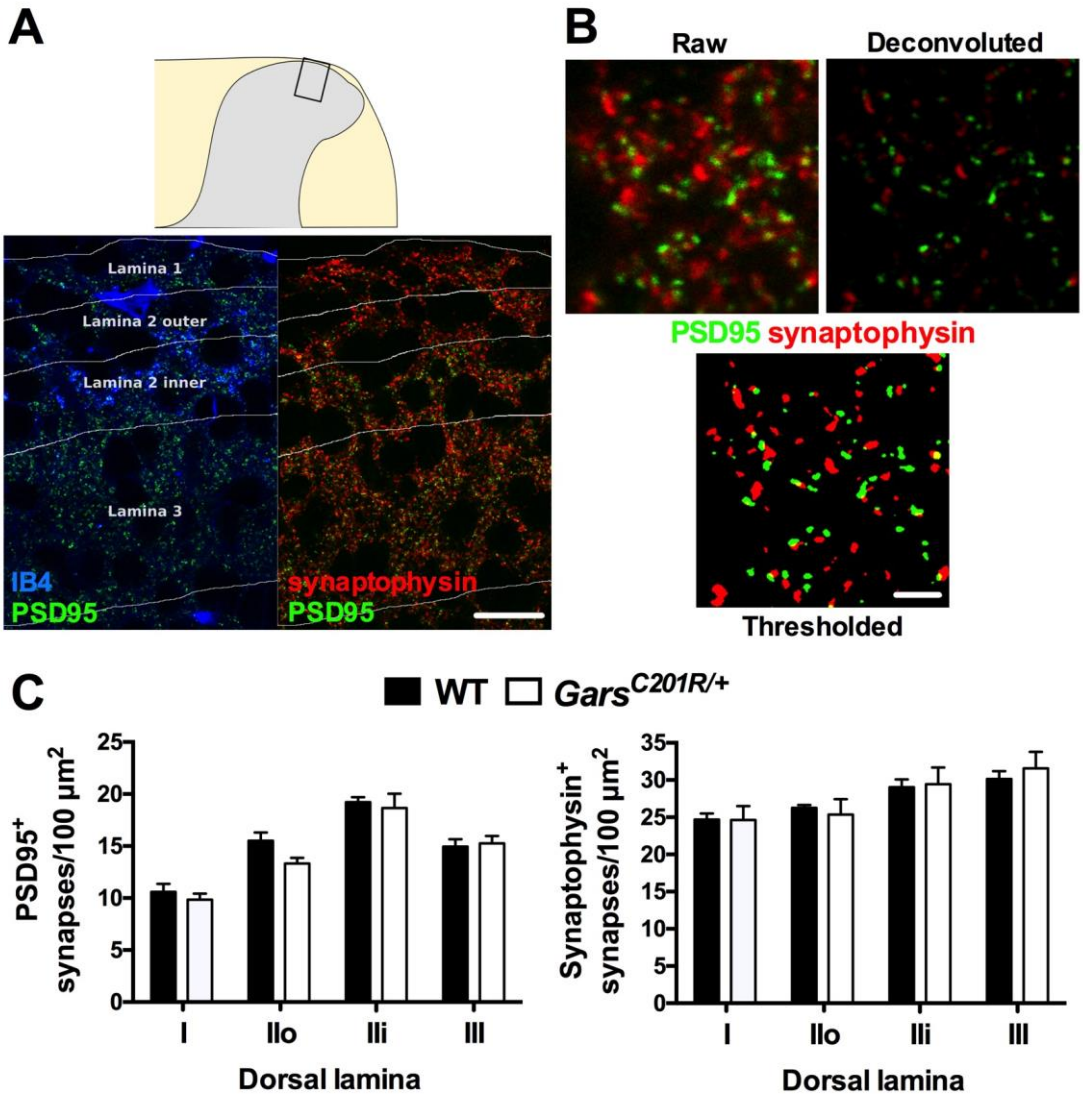

Supplementary Figure 6. Synaptic densities in dorsal horn laminae I-III remain unchanged in one month old *Gars* mice. (A) Representative collapsed z-stack image of a spinal cord section from a one month old wild-type mouse stained for the post-synaptic marker PSD95 (green, bottom), the pre-synaptic protein synaptophysin (red, bottom right), and IB4 (blue, bottom left) to identify lamina II and delineate regions of interest. The schematic (top) depicts the region of the dorsal horn that was imaged. **(B)** Representative images of the deconvolution and thresholding processes used to analyse synapse numbers in distinct laminae (see methods). **(C)** There is no difference in

synapse density in dorsal horn laminae I-III between wild-type and *Gars*$^{C201R/+}$ mice when using either PSD95 (two-way ANOVA, $P < 0.001$, lamina; $P = 0.170$, genotype; $P = 0.472$, interaction) or synaptophysin (two-way ANOVA, $P = 0.002$, lamina; $P = 0.847$, genotype; $P = 0.908$, interaction) to assess synapse numbers. Intra-laminae comparisons between genotypes also show no difference ($P > 0.05$, Sidak's multiple comparisons test). IIo and IIi, outer and inner regions of lamina II, respectively. $n = 4$. Scale bars = 20 μm (A) and 2 μm (B).

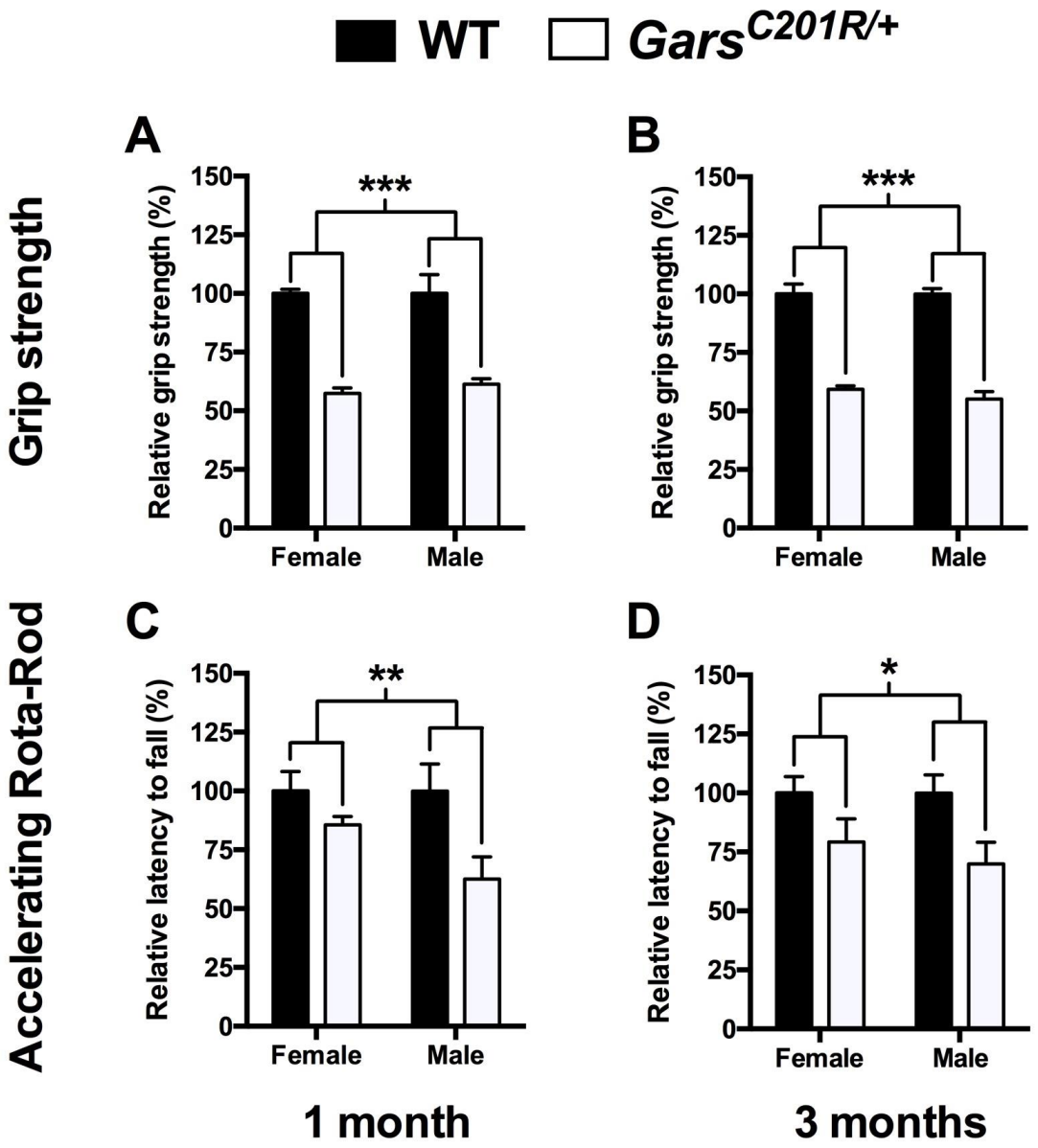

Supplementary Figure 7. *Gars*$^{C201R/+}$ mice display motor defects that remain relatively stable from one to three months. (**A-B**) Both female and male *Gars*$^{C201R/+}$ mice show a significant reduction in grip strength compared to wild-type mice of the same sex at one (A, two-way ANOVA, $P = 0.854$, sex; *** $P < 0.001$, genotype; $P = 0.616$, interaction) and three (B, two-way ANOVA, $P < 0.001$, sex; *** $P < 0.001$, genotype; $P = 0.037$, interaction) months. (**C-D**) Similarly, *Gars*$^{C201R/+}$ mice show a significant reduction in the time taken to fall off an accelerating Rota-Rod at one (C,

two-way ANOVA, $P = 0.326$, sex; ** $P = 0.007$, genotype; $P = 0.188$, interaction) and three months (D, two-way ANOVA, $P < 0.001$, sex; * $P = 0.010$, genotype; $P = 0.972$, interaction). In both behavioural tests, the mutant defects remained relatively stable from one to three months (female grip strength, $P = 0.523$; male grip strength, $P = 0.155$; female Rota-Rod, $P = 0.556$; male Rota-Rod, $P = 0.590$, unpaired *t*-test). The statistical tests of significance represented on the figures were performed on raw data (Supplementary Tables 8 and 9), while the percentages relative to wild-type, which are plotted, were used to compare mutant progression over time. $n = 6$.

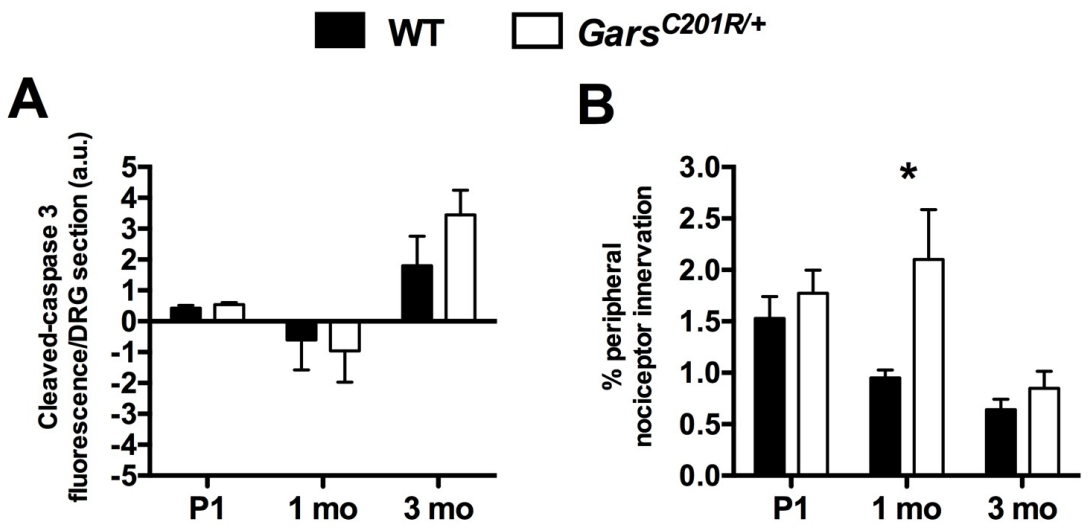

Supplementary Figure 8. Longitudinal analysis of cell death in lumbar DRG and intraepidermal nerve fibre density in glabrous hind paw. (**A**) There is no difference in the cleaved-caspase 3 fluorescence intensity per neuron between wild-type and *Gars*$^{C201R/+}$ DRG at any time point tested, suggesting that cell death is not accounting for the observed DRG cellular phenotype. Two-way ANOVA ($P < 0.001$, age; $P = 0.444$, genotype; $P = 0.413$, interaction). 1 mo, 1 month; 3 mo, 3 months. (**B**) PGP9.5 staining in the hind paw epidermis of wild-type mice decreases progressively from P1 to three months. *Gars*$^{C201R/+}$ mice show no difference at P1, significantly more innervation at one month, but then no difference again at three months. Two-way ANOVA ($P = 0.002$, age; $P = 0.013$, genotype; $P = 0.132$, interaction). * $P < 0.05$, ** $P < 0.01$, Sidak's multiple comparisons test. $n = 3$-5 (A) and 4-6 (B). Data from the one month time point in panels A and B are taken from Fig. S3B and Fig. 3E, respectively.

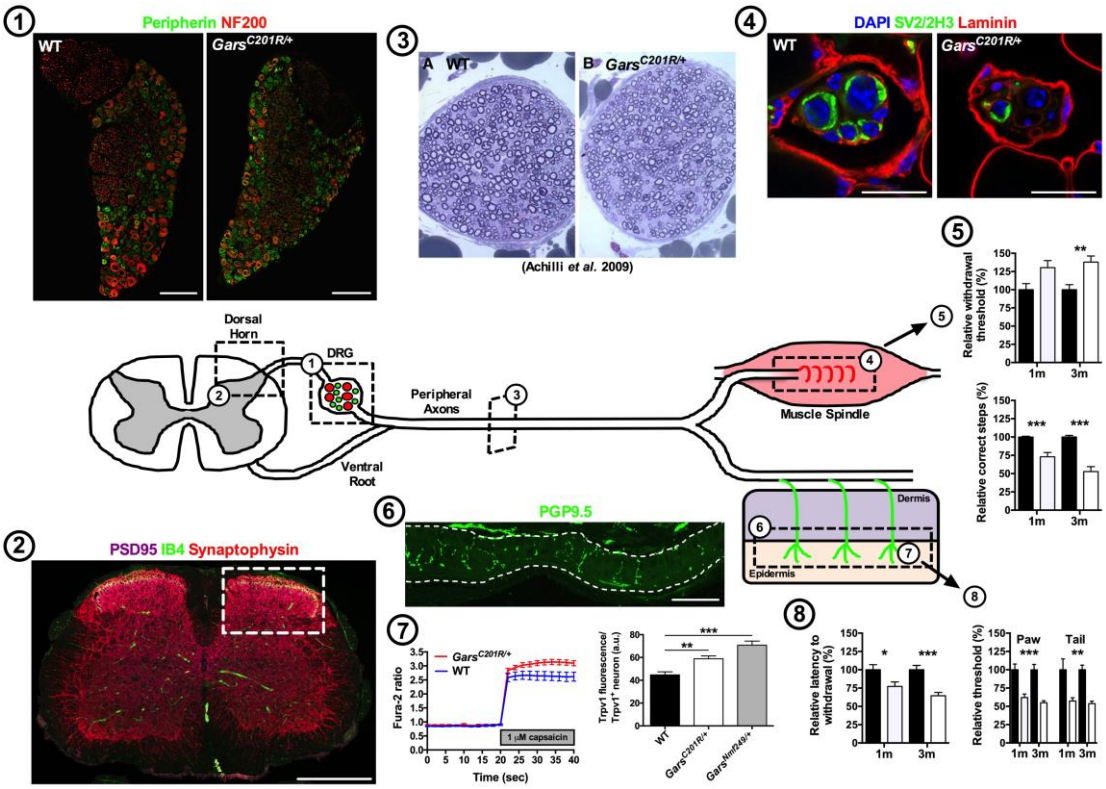

Supplementary Figure 9. CMT2D sensory nervous system pathology. *Gars* mutations distort the proportions of sensory neuron subpopulations in the DRG, such that mutant mice have fewer medium-large (red, NF200^{+}) and more small (green, peripherin^{+}) area neurons from birth to at least three months **(1)**. This does not affect synapse numbers within distinct spinal cord dorsal laminae **(2)**, but may account for the previously reported (2) reduced axon calibre of sensory nerves **(3)** and the diminished number and innervation of muscle spindles in the soleus **(4)**, both of which likely contribute to mutant mechanosensation and proprioception deficiencies **(5)**. Furthermore, mutant *Gars* nociceptors show delayed pruning in peripheral tissue **(6)**, hyperexcitability likely due to increased TRPV1 expression **(7)**, and increased sensory nerve action potential (SNAP) amplitudes, as previously reported (2) (not shown). These phenotypes may explain the pain hypersensitivity observed in *Gars* mice **(8)**. Together, our work indicates that CMT2D may arise from the intricate interaction

between subverted neurodevelopment and neurodegeneration. Scale bars = 100 μm **(1)**, 50 μm **(2** and **6)**, and 20 μm **(4)**. The unaltered pictures of transverse sensory nerves **(3)** were taken from Achilli *et al.* 2009 (2) with permission under the Creative Commons Attribution (CC-BY 3.0) license (http://creativecommons.org/licenses/by/3.0/).

Supplementary Tables

Antigen	Source (Product #)	Host species (clonality)	Concentration used								
			DRG culture	DRG	Skin axon	Muscle spindle	Spinal cord	E18.5 brain	E13.5 feet	N2a cells	WB
CGRP	ELS (BML-CA1137)	Sheep (P)	-	1/200	-	-	-	-	-	-	-
ChAT	Merck AB144P	Goat (P)	-	-	-	-	1/100	-	-	-	-
C-C3	CST (9661)	Rabbit (P)	1/500	1/500	-	-	-	1/500	-	-	-
ERK1/2	CST (9102)	Rabbit (P)	-	-	-	-	-	-	-	-	1/1,000
p-ERK1/2	CST (9101)	Rabbit (P)	-	-	-	-	-	-	-	-	1/500
FLAG	Sigma (F1804)	Mouse (M)	-	-	-	-	-	-	-	1/500	-
GAPDH	Merck (MAB374)	Mouse (M)	-	-	-	-	-	-	-	-	1/3,000
Laminin	Sigma (L9393)	Rabbit (P)	-	-	-	1/1,000	-	-	-	-	-
NeuN	Abcam (ab177487)	Rabbit (M)	-	-	-	-	1/500	-	-	-	-
NF200	Sigma (N0142)	Mouse (M)	1/500	1/500	Failed 1/500	-	-	-	-	-	1/1,000
Parvalbumin	Swant (PV 27)	Rabbit (unknown)	-	1/1000	-	Failed 1/500	-	-	-	-	-
Peripherin	Merck (AB1530)	Rabbit (P)	Failed 1/500	1/500	Failed 1/500	-	-	-	-	-	1/1,000
PGP9.5	UltraClone (RA 95101)	Rabbit (P)	-	-	1/1,000	-	-	-	-	-	-
PSD95	FI (Af628)	Rabbit (P)	-	-	-	-	1/200	-	-	-	-
SV2	DSHB (concentrate)	Mouse (M)	-	-	-	1/250	-	-	-	-	-
Syp	FI (Af300)	Guinea Pig (P)	-	-	-	-	1/200	-	-	-	-

TrkB	Merck (07-225)	Rabbit (P)	-	-	-	-	-	-	-	1/500	1/1,000
TRPV1	Alomone (ACC-030)	Rabbit (P)	-	1/500	-	-	-	-	-	-	-
βIII-tubulin	Abcam (ab41489)	Chicken (P)	1/500	1/500	-	-	-	-	-	-	-
βIII-tubulin	Covance (mms-435p)	Mouse (M)	-	1/500	-	-	-	-	-	-	-
V5	Invitrogen (R960CUS)	Mouse (M)	-	-	-	-	-	-	-	-	1/3,000
2H3	DSHB (supernatant)	Mouse (M)	-	-	-	1/250	-	-	1/50	-	-

Supplementary Table 1. Primary antibodies successfully used for immunofluorescence and western blotting. 2H3, neurofilament; C-C3, cleaved-caspase 3; CST, Cell Signaling Technology; DSHB, Developmental Studies Hybridoma Bank; ELS, Enzo Life Sciences; FI, Frontier Institute; GAPDH, glyceraldehyde-3-phosphate dehydrogenase; M, monoclonal; P, polyclonal; Syp, synaptophysin; SV2, synaptic vesicle 2; WB, western blot. For failed staining, the highest concentration is reported.

Antigen	Source	Host species	Concentration used

	(Product #)	(clonality)	DRG	Muscle spindle	N2a cells
Parvalbumin	Swant (PV 235)	Mouse (M)	Failed 1/500	Failed 1/500	-
Parvalbumin	Swant (PVG-213)	Goat (unknown)	1/500	Failed 1/500	-
Peripherin	Merck (MAB1527)	Mouse (M)	1/200	-	-
Peripherin	Santa Cruz (sc-28539)	Rabbit (P)	Failed 1/50	-	-
Runx3	Abnova (864-A01)	Mouse (P)	Failed 1/100	-	-
TrkB	BD (610101)	Mouse (M)	-	-	1/500
Vglut1	Merck (AB5905)	Goat (P)	-	Failed 1/1,000	-

Supplementary Table 2. Additional primary antibodies tested in the study. BD, BD Biosciences; M, monoclonal; P, polyclonal. For failed staining, the highest concentration tested is reported.

	von Frey withdrawal threshold (g)	
Age (months)	Wild-type	*Gars*$^{C201R/+}$
1	0.38 ± 0.028	0.48 ± 0.035
3	0.49 ± 0.035	0.66 ± 0.041**

Supplementary Table 3. Raw data generated by the von Frey test of mechanosensation at one and three months. ** $P < 0.01$, compared to wild-type using Sidak's multiple comparisons test.

	% correct steps in beam-walking test	
Age (months)	Wild-type	*Gars*$^{C201R/+}$
1	94.1 ± 1.0	68.7 ± 5.5***
3	88.7 ± 2.0	46.8 ± 5.9***

Supplementary Table 4. Raw data generated by the beam-walking test of proprioception at one and three months. *** $P < 0.001$, compared to wild-type using Dunn's multiple comparison test.

	Randall-Selitto paw threshold (g)	
Age (months)	Wild-type	*Gars*$^{C201R/+}$
1	123.3 ± 9.6	76.5 ± 5.9***
3	135.2 ± 9.9	74.3 ± 3.6***

Supplementary Table 5. Raw data generated by the Randall-Selitto test of hind paw mechanical nociception at one and three months. *** $P < 0.001$, compared to wild-type using Sidak's multiple comparisons test.

	Randall-Selitto tail threshold (g)	
Age (months)	Wild-type	*Gars*$^{C201R/+}$
1	104.1 ± 15.3	59.6 ± 4.6**
3	153.0 ± 9.6	81.9 ± 5.2***

Supplementary Table 6. Raw data generated by the Randall-Selitto test of tail mechanical nociception at one and three months. ** $P < 0.01$, *** $P < 0.001$, compared to wild-type using Sidak's multiple comparisons test.

	Hargreaves latency to withdrawal (s)	
Age (months)	Wild-type	*Gars*$^{C201R/+}$
1	7.06 ± 0.53	5.44 ± 0.46*
3	9.03 ± 0.53	5.84 ± 0.41***

Supplementary Table 7. Raw data generated by the Hargreaves test of thermal nociception at one and three months. * $P < 0.05$, *** $P < 0.001$, compared to wild-type using Sidak's multiple comparisons test.

	Grip strength (g)			
	Female		Male	
Age (months)	Wild-type	*Gars*$^{C201R/+}$	Wild-type	*Gars*$^{C201R/+}$
1$^{###}$	156.3 ± 2.8	89.7 ± 3.6***	154.1 ± 12.3	94.4 ± 3.7***
3$^{###}$	234.3 ± 9.9	138.8 ± 3.5***	289.8 ± 6.6	159.7 ± 9.3***

Supplementary Table 8. Raw data generated by the grip strength test at one and three months. *** $P < 0.001$, compared to wild-type using Sidak's multiple comparisons test. ### $P < 0.001$, two-way ANOVA comparison of genotypes.

	Latency to fall (s) on accelerating Rota-Rod			
	Female		Male	
Age (months)	Wild-type	*Gars*$^{C201R/+}$	Wild-type	*Gars*$^{C201R/+}$
1$^{\#\#}$	130.8 ± 10.8	112.0 ± 4.7	134.9 ± 15.5	84.5 ± 12.7*
3$^{\#}$	128.3 ± 8.9	101.6 ± 12.7	86.5 ± 6.7	60.5 ± 8.0

Supplementary Table 9. Raw data generated by the accelerating Rota-Rod test at one and three months. * $P < 0.05$, compared to wild-type using Sidak's multiple comparisons test. $^{\#}$ $P < 0.05$, $^{\#\#}$ $P < 0.01$, two-way ANOVA comparison of genotypes.